Foot-Healthcare Application Using Inertial Sensor: Estimating First Metatarsophalangeal Angle From Foot Motion During Walking

Chenhui Huang, *Member, IEEE*, Kenichiro Fukushi, Zhenwei Wang, Hiroshi Kajitani, Fumiyuki Nihey, Hannah Pokka, Hiroko Narasaki, Hiroaki Nakano, and Kentaro Nakahara

***Abstract*—Our purpose was to demonstrate the possibility of providing foot-healthcare application by using an in-shoe motion sensor (IMS) through validating the feasibility of applying an IMS for measuring the first metatarsophalangeal angle (FMTPA), which is the most important parameter regarding the common foot problem hallux valgus. Methods: The IMS signals can represent foot motions when the mid-foot and hindfoot were modelled as a rigid body. FMTPAs can be estimated from the foot-motion signals measured using an IMS embedded beneath the foot arch near the calcaneus side using a machine-learning method. The foot-motion signals were collected from 50 participants with different FMTPAs. The true FMTPAs were assessed from digital photography. Correlation-based feature-selection processes (significance level $p < 0.05$) were used to search for the predictors from the foot-motion signals. Leave-one-subject-out cross-validation, root mean squared error, and intra-class coefficients were used for FMTPA-estimation model evaluation. Results: Eleven FMTPA-impacted gait-phase clusters, which were used to construct effective foot-motion predictors, were observed in all gait-cycle periods except terminal swing. The range of the foot motion in the sagittal and coronal planes significantly correlated with the FMTPA ($p < 0.05$). Linear regression could be the best method for constructing an FMTPA estimation model with a root mean squared error and intra-class correlation coefficient of 4.2 degrees and 0.789, respectively. Conclusion: The results indicate the reliability of our FMTPA estimation model constructed from foot-motion signals and the possibility to providing foot-healthcare applications by using an IMS.**

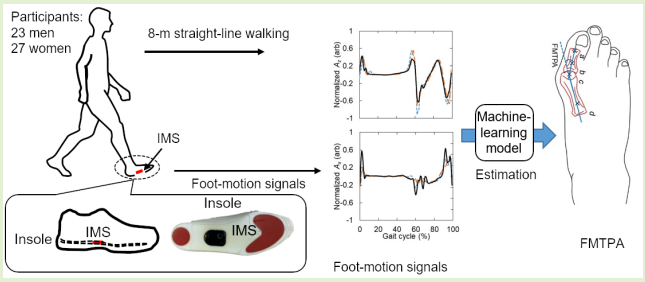

***Index Terms*—Inertial sensor, foot-motion, foot health, gait analysis, hallux valgus.**

I. Introduction

With the development of Internet-of-Things technologies, wearable smart sensors, which can finish all the data processing on an edge device, have been applied to various healthcare applications by automatically recording biomedical signals, such as pulse and sweat, in daily living without intentional manipulation [1], [2]. The relationship between walking and health has been receiving attention. There are mainly two types of wearable smart sensors believed to have high potential for health applications through daily gait analysis. One is smart sensors using optical sensing technology [3] and the other is smart motion sensors [4]. Placing a sensor in various shoes or insoles is now considered promising for providing various healthcare applications in a more convenient manner because it is less of a hassle to wear and enables automatic recording and analyzing of foot motions during daily walking. Examples of smart wearable optical sensors are smart insoles integrated with polymer optical fibers [5], [6], which were developed for measuring ground-reaction force and foot pressure during walking. They are low cost, portable, and have a high degree of customizability and high potential for clinical evaluation and remote health

Manuscript received December 1, 2021; accepted December 18, 2021. Date of publication December 24, 2021; date of current version January 31, 2022. The associate editor coordinating the review of this article and approving it for publication was Prof. Danilo Demarchi. *(Corresponding author: Chenhui Huang.)*

This work involved human subjects or animals in its research. Approval of all ethical and experimental procedures and protocols was granted by the NEC Ethical Review Committee for the Life Sciences under Protocol No. LS2019-010.

Chenhui Huang, Kenichiro Fukushi, Zhenwei Wang, Hiroshi Kajitani, Fumiyuki Nihey, and Kentaro Nakahara are with the Biometrics Research Labs, NEC Corporation, Abiko, Chiba 270-1174, Japan (e-mail: chenhui.huang@nec.com; k-fukushi@nec.com; w-zhenwei@nec.com; h-kajitani@nec.com; nihey@nec.com; k-nakahara@nec.com).

Hannah Pokka, Hiroko Narasaki, and Hiroaki Nakano are with the Business Innovation Unit, NEC Corporation, Minato City, Tokyo 108-8001, Japan (e-mail: h-jin@nec.com; narasaki@nec.com; hiroaki.nakano@nec.com).

Digital Object Identifier 10.1109/JSEN.2021.3138485

monitoring [5], [6]. Although such sensors are sensitive to temperature [7], as long as this is taken into account, the gait information of all subdivisions of the stance phase can be evaluated [5]. A new type of wearable smart motion sensor, called an "in-shoe motion sensor (IMS)", is considered promising for enabling various healthcare applications for daily walking. An IMS automatically records and analyzes foot motions not only in the stance phase but during the entire gait cycle (GC) during daily walking [8]–[10].

The combination of smart motion sensors for measuring gait parameters with artificial intelligence (AI) technologies has been reported both for monitoring short-term changes in daily physical conditions, e.g., effect of daily exercise or physical fatigue [11], [12], and predicting long-term changes, e.g., frailty or Parkinson's disease, using signal features from daily gait monitoring [13], [14]. Foot problems significantly impact the quality of life, particularly the quality of ambulatory life [15]–[17]. Monitoring foot health is believed a necessary [18], [19]. We argue that an IMS is a promising option for providing convenient daily foot-health monitoring, however, to the best of our knowledge, there has been little research on foot-health monitoring using only foot motions; thus, the feasibility of using an IMS to monitor foot health should be verified. To do this, we focused on hallux valgus (HV), which is a common toe deformity today [17], [20].

When the first metatarsophalangeal angle (FMTPA) continuously increases, HV will occur. Extrinsic factors including an inappropriate choice of shoes and inappropriate walking form are partial causes of HV deformity progression [20]. Although HV will substantially worsen the quality of ambulatory life in its late stage [21], it is usually easy to ignore or incurs no pain in the early stage [22]. In other words, if the most essential parameter for HV deformity assessment, FMTPA, is frequently monitored, i.e. accumulating a large amount of the time-series data, we will be able to use AI technologies to detect the early signs of HV, estimate its current status, or predict risk of HV progression by combining it with other gait parameters. This will make it possible to urge those who had not been aware of their HV progression to take action, e.g., by choosing appropriate shoes and doing exercise to improve walking form, or advise those whose HV has progressed to access clinical examinations and treatments.

Machine-learning models are widely used in various applications. There are two essential factors in constructing high-precision machine-learning models. One is the selection of an optimal computational algorithm, and the other is the selection of optimal predictor variables. We focused on the latter for this study. Walking is a natural form of periodic movement in which the lower limbs are moved forward alternatively. The musculoskeletal model [23] revealed that the same musculoskeletal structure is used and the same motion is repeated at the same phase in one GC. Understanding the impact of HV on gait is considered important for assessing the FMTPA [24]. Previous studies reported alterations of kinematics on lower limbs, e.g., more eversion during pre-swing (PS), less external rotation during terminal stance (TSt) on the hindfoot-tibia, and less range of motion of the hindfoot-tibia in the sagittal plane, in people with HV [25]–[27]. By referencing these studies, the gait features of HV can be easily found during straight-path walking. Consequently, we considered that through understanding the impact of FMTPA on foot motion, we can find predictors that intrinsically correlate with the FMTPA from measuring foot motion in specific phases of one GC during straight-path walking.

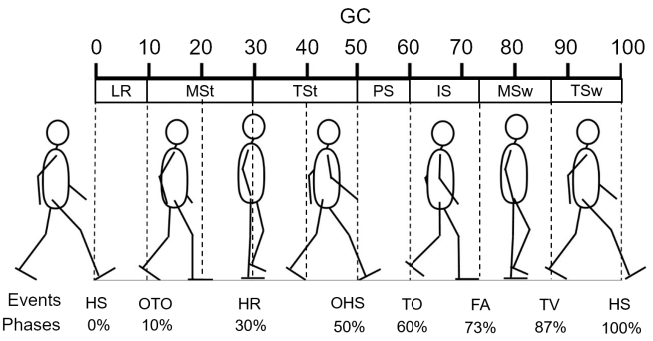

Fig. 1. Schematic of one GC, gait phases, and gait events.

We previously reported the impact of HV on inertial foot-motion signals measured using an IMS [28]. In this paper, we first present analysis on the data obtained from participants with different FMTPAs to understand which phases of foot-motion are impacted by FMTPA. We then discuss determining predictor variables from these FMTPA-impacted gait phases, and constructing machine-learning models for estimating the FMTPA. Finally, we present FMTPA estimation results obtained after inputting foot-motion signal features into the constructed models.

II. Gait Cycle

One GC is the time period or sequence of events or movements during locomotion in which one foot contacts the ground to when that same foot again contacts the ground. The motion of a foot contacting the ground is called heel strike (HS), which is one of seven defined gait events, i.e. special motion during walking. One GC can be partitioned into stance and swing phases at toe off, which comprise 60 and 40% of a GC, respectively, as shown in Fig. 1 (taking the right foot as an example). One GC can be divided into seven periods: loading response (LR), mid-stance (MSt), terminal stance (TSt), pre-swing (PS), initial swing (ISw), mid-swing (MSw), and terminal swing (TSw) on the basis of six other gait events in one GC: opposite toe off (OTO), heel rise (HR), opposite heel strike, toe off (TO), feet adjacent, and tibia vertical, respectively [23].

III. Materials and Methods

A. Participants

We recruited 50 participants (23 men and 27 women) of different ages, heights, weights, and shoe sizes for our experiment. The average age, height, weight, and shoe size were 48.4 $\pm$ 8.5 years, 165.0 $\pm$ 6.9 cm, 60.1 $\pm$ 10.3 kg, and 24.8 $\pm$ 1.2 cm, respectively. The dominant leg was judged as the side of the leg used for taking the first-step forward [29], where the ratio of left to right was 20:30. All participants could walk independently without any assistive devices. They had normal or corrected-to-normal vision, no history

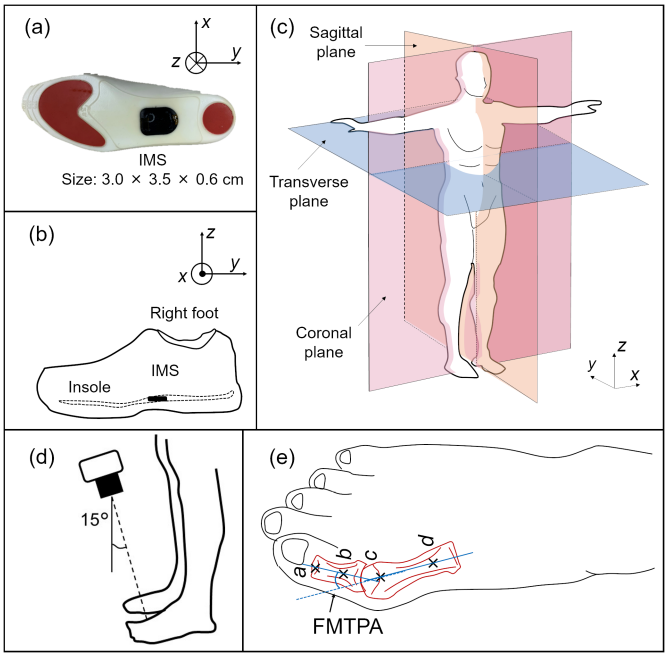

Fig. 2. (a) Schematic of IMS embedded in insole; (b) schematic of insole inserted in sports shoe; (c) definition of coordinate axes and corresponding plane with directions defined as A_x (medial: +, lateral: −), A_y (posterior: +, anterior: −), A_z (superior: +, inferior: −), G_x (plantarflexion: +, dorsalflexion: −), G_y (eversion: +, inversion: −), G_z (adduction: +, abduction: −), E_x (plantarflexion: +, dorsalflexion: −), E_y (eversion: +, inversion: −), and E_z (adduction: +, abduction: −); (d) camera setup for photographic FMTPA assessment; and (e) measurement method of FMTPA from digital photography. Points *a* and *b* were marked at visual bisection points at distal and proximal shaft of proximal. Point *c* was located at center of first metatarsal head, and Point *d* was marked at visual bisection of proximal first metatarsal shaft.

of neuromuscular or orthopedic diseases, and no obstacles to communication. The experimental procedure was explained to all participants, and informed consent was obtained from each individual before the experiment. The study was approved by the NEC Ethical Review Committee for the Life Sciences (protocol number: LS2019-010) on Sep. 11, 2019.

B. Experimental Setup and Protocol

An IMS was embedded in an insole placed under the foot arch near the calcaneus side to ensure that participants could walk naturally, and the insole was inserted into sports shoes (Figs. 2(a) and (b)). The data were transferred to a smartphone using Bluetooth Universal Asynchronous Receiver/Transmitter (UART) in real time. The communication-capacity limitation allowed us to use only one IMS for one participant during measurement. Because foot motion is assumed to be symmetric between the dominant and non-dominant leg, we used the IMS for only the right foot.

When the shoes fit tightly and mid-foot and hindfoot were modelled as a rigid body, the signal from the IMS in the shoes could be assumed to be equal to the foot-motion signals. The IMS contained a 6-axis inertial measurement unit (IMU) (BMI 160, Bosch Sensortec, Germany), general-purpose multiprotocol system-on-chip (nRF52832, Nordic Semiconductor, Norway), and control circuit. Nine types of foot-motion signals, including three axes of acceleration, i.e., linear motions A_x, A_y, and A_z and angular velocity, i.e., rotating motions G_x, G_y, and G_z, were directly measured. Inside a microcomputer, the three axes of sole-to-ground angles E_x, E_y, and E_z were calculated using a Madgwick filter [30], and the acceleration values were then corrected to the global coordinates automatically.

The participants walked in 8-m straight lines for eight successive trials at a self-determined comfortable speed. Before data collection, the participants were given a 2-min practice session to familiarize themselves with the environment and procedure. The data-sampling frequency of the IMS was set to 100 Hz. The measurement range of acceleration was ±16 g, and the angular velocity was ±2000 degree/s.

C. FMTPA: Target Variables

The true FMTPA in this study was obtained using a photographic method that has been shown to be valid for self-checks of HV as long as the photographing conditions including photographing position, angle, and standing posture are rigorously adjusted [31]. We used the camera on an iPhone (Apple, USA), which was set at 15 degrees from the perpendicular axis and guided using a tripod (Fig. 2(d)). The participants were instructed to stand erect and look forward. From the photo, reference points a, b, c, and d, were marked. The FMTPA was calculated using the intersection of two axes, a-b and c-d (Fig. 2(e)). The principal examiner determined the reference points and took measurements from all photographs on three separate occasions with a one-month interval between each. That is, on each measurement occasion, each image was independently marked up, and independent measurement was conducted. To minimize test-retest bias and ensure that the examiner was unable to recall previous observations, no reference was made to the data or images in the interim. Finally, the FMTPA of each participant was obtained by averaging the three separate measurements.

D. Data Processing

The IMS signals of each trial were split into strides by detecting an HS event from A_y on the basis of the gait-event-detection algorithm in our previous study [32]. Approximately 50 effective strides of each participant were selected from the database. Note that the first and last strides of each walking trial and those strides including outlier values, e.g. defective data due to communication packet loss or decoding error, etc. were excluded. Foot kinematics is affected by walking velocity [33]; to exclude the velocity bias on foot motion, the amplitude of acceleration and angular velocity waveform of every stride were normalized using the corresponding maximum instantaneous walking velocity during the swing phase, which was calculated by integrating A_y from a foot flat to the end of the stride. Each stride was then temporally normalized to a 1–100 percentage gait cycle (%GC), as a result, the data of every normalized stride formed a 100 × 9 matrix. The data in the columns mean the data of 1–100 %GC of A_x, A_y, A_z, G_x, G_y, G_zE_x, E_y, and E_z. Next, all normalized strides of each participant were averaged as the average foot motion of each participant. Finally, each participant had one average

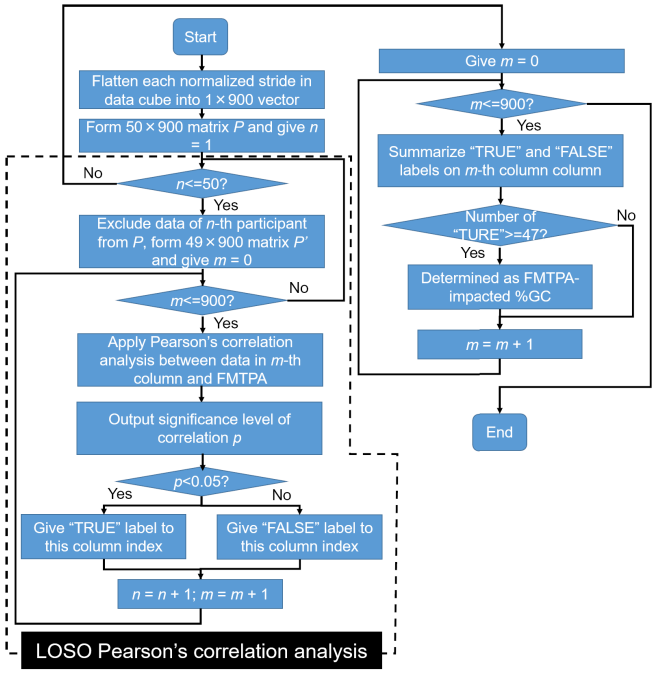

Fig. 3. Flow chart of analysis for observing FMTPA-impacted gait phase.

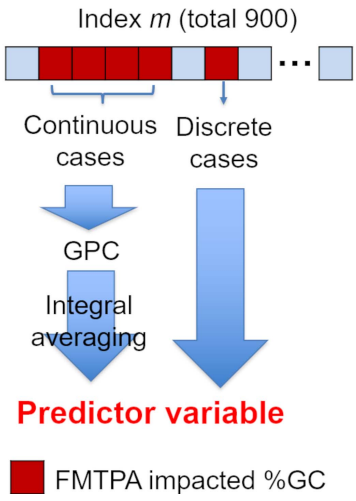

Fig. 4. Schematic of FMTPA-impacted %GC.

foot motion, and a total of 50 datasets were used for model construction and evaluation, which formed a 100 × 9 × 50 data cube. The noise levels (NLs) of the IMS signals were also measured while the IMS was placed on a desk.

E. Feature Selection

In this section, we explain the processes to analyze which phases in one GC were significantly impacted by FMTPA, as shown in Fig. 3.

As the preprocessing, each averaged normalized stride in the data cube was flattened into a 1 × 900 vector, turning the data cube into a 50 × 900 matrix P. Correlation analysis with the leave-one-subject-out (LOSO) process was used in the feature selection to avoid overfitting. The data of the n-th participant were first excluded, where n is the participant number, and the data of the remaining 49 participants were used for the analysis, forming a 49 × 900 matrix P'. Pearson's correlation analysis was used to examine whether there was significant correlation between the amplitude of normalized foot-motion signals and the FMTPA at every 1%GC. The inputs were the data of the m-th column of P' and the FMTPA, where m is a number between 1 and 900, and the output was the level of significance of correlation analysis. If the level of significance of correlation was $p < 0.05$, a "TRUE" label was given to m; if not, a "FALSE" label was given. The Pearson product moment correlation coefficient r of m was also recorded as a reference value. The LOSO process was repeated 50 times because there were 50 participants in our study. "TRUE" or "FALSE" labels were also given 50 times to every m. The labels on every m were then summarized. Those indexes with over 47 "TRUE" labels were considered intrinsically correlating with the FMTPA, i.e., as FMTPA-impacted %GC, despite individual differences.

Predictor variables were processed from the data of FMTPA-impacted %GC for constructing a regression model. The target variables of the regression model were FMTPAs. As shown in Fig. 4, a group of continuous FMTPA-impacted %GCs were treated as a cluster, which was called a "gait phase cluster (GPC)", and the integral average of the signal amplitude in the GPC, i.e., the average motion intensity of each GPC, was output as a single predictor, while the signal amplitude at each non-continuous FMTPA-impacted %GC was directly guided as a predictor. Of course we can treat every FMTPA-impacted %GC as independent predictors. However, because foot motion is temporally successive, we considered that the integral average value can represent foot motion during those GPCs, which is considered more biomechanically interpretable, as well as helpful to reduce the number of predictors. The variance inflation factor (VIF) was used to test the multicollinearity, the threshold of which was set to 10.

F. Estimation Model Construction and Evaluation

We used MATLAB (Mathworks, USA) to execute all data processing and model construction. Because of the small dataset, after predictor variables were determined, we preferentially conducted a linear regression method for prediction then compared it with five other classical machine-learning regression methods: support vector machine, Gaussian process regression, random forest, decision tree and neural network, which are easily available on MATLAB toolbox.

Leave-one-subject-out cross-validation (LOSOCV) was used for the model evaluation, and the root mean squared error (RMSE), intra-class correlation coefficients (ICCs) of type (2, k), and Bland-Altman plots were used for evaluating the precision of the estimated results, levels of agreement between the measured and estimated results, and limit of agreement between both systems. The guidelines for interpreting ICC inter-rater agreement were excellent (>0.900), good (0.750–0.899), fair (0.500–0.749), and poor (<0.500) [34].

IV. Results

A. FMTPA-Impacted %GCs

The FMTPA-impacted %GCs were found in the linear motion of all directions (A_x, A_y, and A_z) and in the

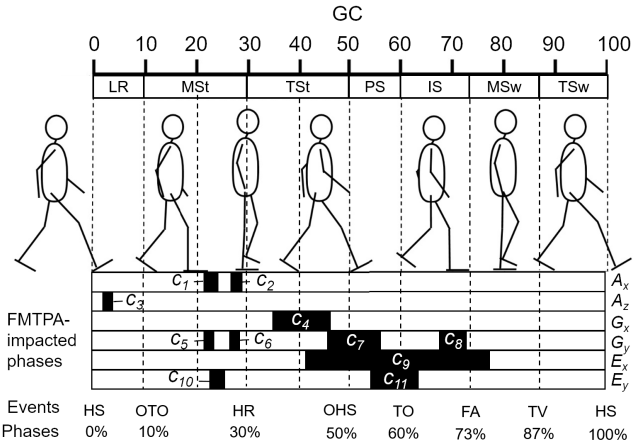

Fig. 5. Schematic of FMTPA-impacted %GCs gait phase (black blocks in lower part) listed in Table I.

TABLE I
DETAILS OF FMTPA-IMPACTED %GCS

Signal type	Cluster number	Impacted %GCs	Description of gait phases and corresponding motion
A_x	c_1	22–24	Early MSt, foot flat
	c_2	27–29	Late MSt, foot flat
A_z	c_3	3–4	Immediately after HS
G_x	c_4	35–46	TSt, HR
G_y	c_5	22–23	Early MSt, foot flat
	c_6	27–28	Late MSt, foot flat
	c_7	46–56	Late TSt to PS
	c_8	68–72	Late ISw
E_x	c_9	41–77	TSt to the end of MSw
E_y	c_{10}	23–25	Early MSt, foot flat
	c_{11}	54–63	Immediately before and after TO

rotational motion and sole-to-ground angle (SGA) in the sagittal (G_x and E_x) and coronal (G_y and E_y) planes. None were found in the transverse plane (G_z and E_z). Eleven GPCs were found (c_1–c_{11}), and their details are shown in Table I and Figs. 5 and 6.

The FMTPA impacted almost the same %GCs of MSt (c_1, c_5, and c_{10}; c_2 and c_6) on both the linear and rotational motions in the coronal plane. Immediately after an HS and before a foot flat, the %GCs approaching a signal peak in A_z were affected (c_3). Combined with c_4, c_7, and c_{11}, the FMTPA affected the rotational velocity and SGA in the sagittal to coronal planes in order during TSt and PS. The FMTPA also affected the SGA in the sagittal plane throughout the TSt to MSw (c_9), whereas it affected the rotational motion only on TSt for (c_4).

B. Predictor Variables

All the following results are shown in Fig. 7. By measuring from digital photography, we found that the FMTPAs of all participants were 20.7 ± 5.5 degrees, where the maximum was 35.3 degrees and minimum was 10.2 degrees. The range of amplitudes of all predictor variables (C_1–C_{11}) exceeded the NLs. The intensity values of C_2, C_6, and C_8 decreased, while

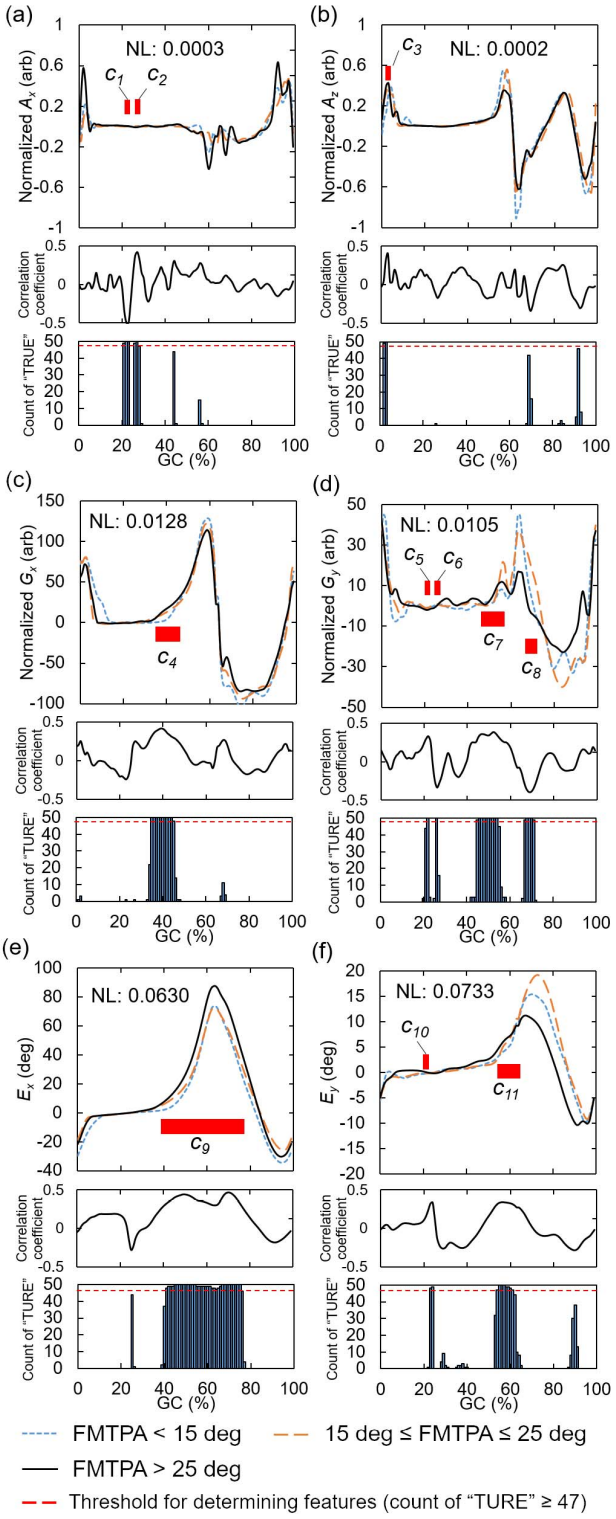

Fig. 6. Different types of foot-motion signals in one GC of three example participants whose FMTPA were below 15 (blue dotted line), between 15 to 25 (orange dashed line), and over 25 degrees (black line) (top column), together with the average correlation coefficient r (middle column) and the numbers of times marked as $p < 0.05$ in every 1% GC (bottom column) counted fifty times for the leave-one-subject-out process, and they are listed as follows corresponding to signal types. (a) A_X; (b) A_Z; (c) G_X; (d) G_Y; (e) E_X; (f); and E_Y. FMTPA-impacted GPCs are denoted as red blocks. Red dashed line (Count = 47) means threshold for determining significant FMTPA-impacted %GC.

TABLE II
EVALUATION OF FMTPA ESTIMATION MODELS USING SIX MACHINE-LEARNING-BASED APPROACHES

Approaches	RMSE (deg)	ICC
Linear regression with the least squares method	4.2	0.789
Support vector machine with linear kernels	4.2	0.754
Gaussian process regression with exponential kernels	4.5	0.663
Random forests	4.8	0.521
Decision tree	4.8	0.583
Neural network	6.8	0.677

those of C_1, C_3, C_4, C_5, C_7, C_9, C_{10}, and C_{11} increased as the FMTPA increased. The trends of C_1 and C_2 also synchronized with those of C_5 and C_6, respectively. The absolute value of r of all the predictors exceeded 0.3, and C_1 had the strongest correlation with the FMTPA, i.e., 0.502. The VIFs of the predictors were all below 10, meaning they could be treated as independent variables.

The inversion of the positive and negative values of C_1, C_2, C_5, and C_6 as the FMTPA increased was indicative of the inversion of the foot-motion direction. Both the linear and rotational motions during early MSt (C_1 and C_5) had changes opposite to those during late MSt (C_2 and C_6). For low FMTPAs, the acceleration vector transited from lateral to medial from early to late MSt, and the feet changed the rotational direction from inversion to eversion. However, for high FMTPA, the transition in the acceleration vector and changing of the feet's rotational direction were completely opposite to those for low FMTPA. The SGA also shifted from inversion to eversion as the FMTPA increased (C_{10}). The linear and rotational motions seemed to be nearly zero when the FMTPA was around 20 degrees. When the FMTPA increased, the feet had more pronated rotation immediately before TO (C_7) as well as more SGA eversion immediately before and after TO (C_{11}). The participants with higher FMTPAs had higher average SGAs in the dorsal-flexion direction from the beginning of TSt to the end of MSw (C_9).

C. Evaluation of Constructed FMTPA Estimation Models

The evaluation results of FMTPA estimation models constructed by linear regression and other machine learning approaches are shown in Table II. The RMSEs in the LOSOCV of four of the methods were very similar, whereas the ICCs showed that linear regression could be the best for constructing an FMTPA estimation model. Its RMSE was 4.2 degrees and ICC was 0.789, suggesting that this estimation model could precisely distinguish between the FMTPA at a resolution of 4.2 degrees, achieving a "good" agreement between the true and estimated values. This indicates that it is possible to achieve rapid prediction directly on an edge device, i.e. IMS, without transferring foot-motion data to servers or clouds, which consumes a large amount of battery power.

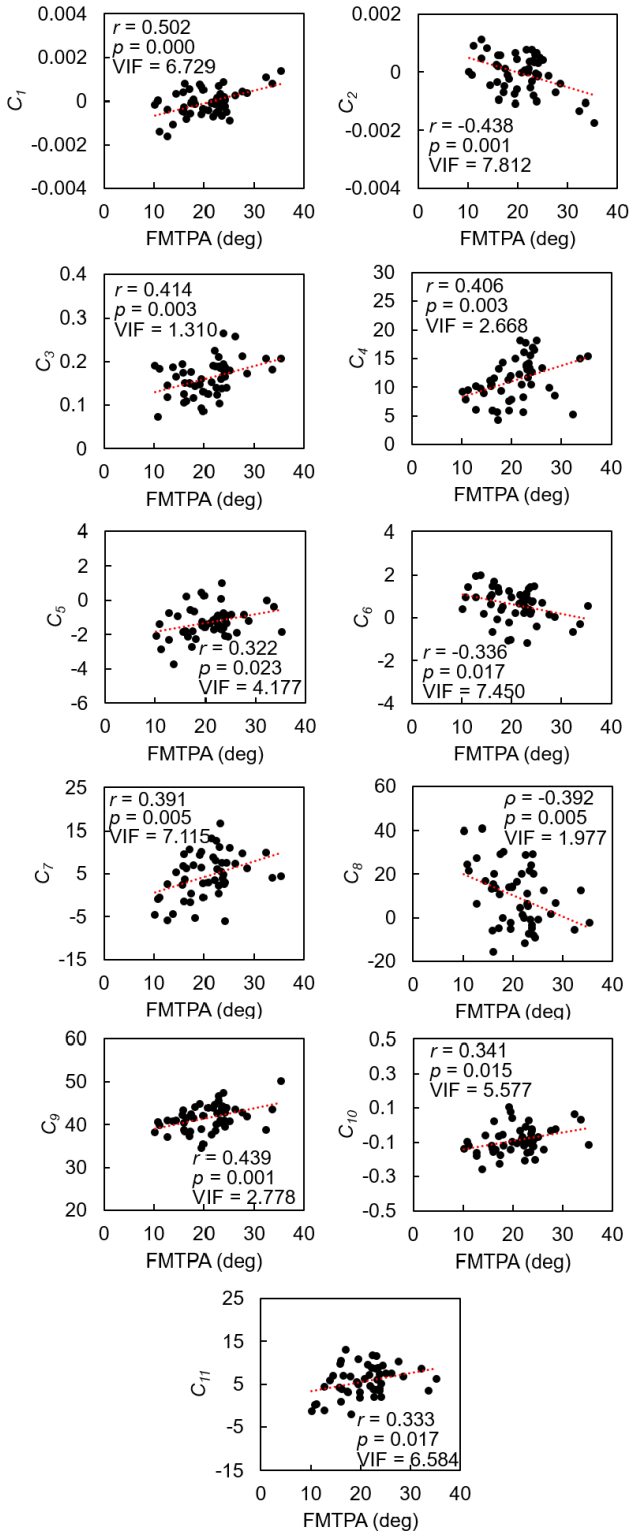

Fig. 7. Correlation coefficient with FMTPA, level of significance, VIF, and trends of predictors. Red dotted line shows fitted trend line from scattered black dots.

Except for several exceedingly high FMTPA points, most of the plots were well scattered around the equivalent line between the true and estimated values (Fig. 8(a)). The estimated values only had a difference of -0.2 ± 4.2 degrees with the true values, and no proportional bias existed between them (Fig. 8(b)).

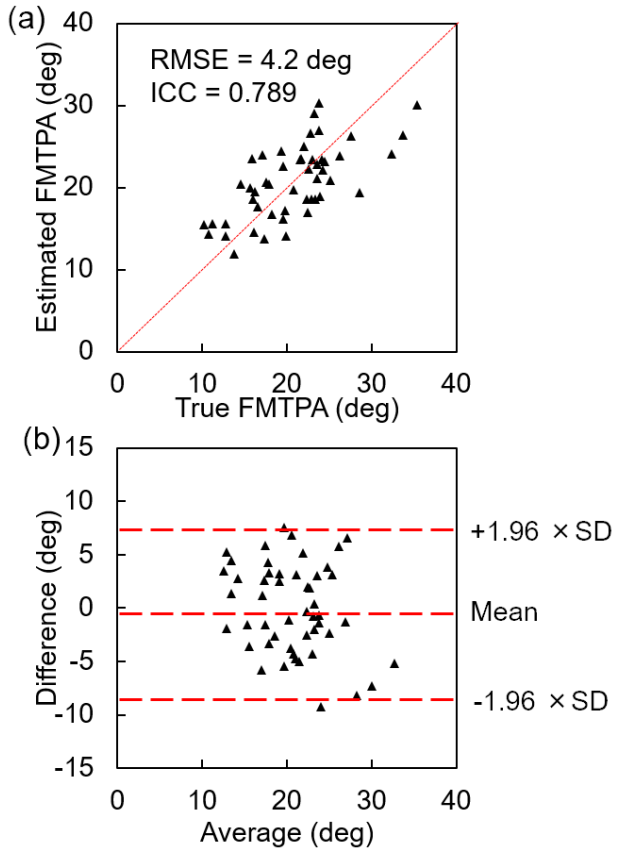

Fig. 8. (a) Agreement test results of the linear regression model between the true and estimated FMTPA values in the LOSOCV; the red dotted line means the equivalent line between the true and estimated value and (b) Bland-Altman plots and the limit of the 95% confidence interval (CI, ±1.96 SD (standard deviation)) around perfect agreement in the comparison of the true and estimated values; the red dashed line in the middle means the mean value, and the top and bottom red dashed lines mean the upper and lower limits of the CI.

V. Discussion

We investigated for the first time the correlation between the FMTPA and foot motion, especially inertial signals that only originate from single segment kinematics relative to the global coordinates when considering forefoot-hindfoot as a rigid body. In a commonly used grading system, the deformities were assessed at an FMTPA as normal (<15 degrees), mild (15–20 degrees), moderate (20–39 degrees), and severe (>39 degrees) [35]. In conventional HV assessment, FMTPA measurements using a goniometer can easily be affected by the presence of swelling, position of the goniometer arms, and skill of the operator. Even when angle measurements are taken from standard radiographs, measurement errors of 5 degrees have been recorded [36]. We believe that our estimation model achieved the same precision level as with the conventional HV assessment method using radiography.

An IMU is sensitive to temperature [37]. In this study, we chose BMI 160, Bosch Sensortec as the IMU integrated in the IMS. According to the datasheet of this type of IMU [38], a temperature sensor was integrated inside the IMS for compensation. For the acceleration measurement, the sensitivity temperature drift was only ±0.03%/K and zero-g offset temperature drift was ±0.001G/K, and for angular velocity measurement, sensitivity change-over temperature was ±0.02%/K and zero-rate offset change-over temperature was 0.05 deg/s/K. Our IMS was packaged in a case made of acrylonitrile butadiene styrene, embedded into an insole made of silicone rubber, and further wrapped by the sole of the shoe after the insole was inserted into the shoe (also see Fig. 2(b)). When a user wears the shoe, the IMU will be located in a closed operation environment close to the body; thus, we considered the temperature change surrounding the IMU should be no more than 0.5K and compared with C_1 to C_{11}, its impact can be ignored when estimating the FMTPA.

Through LOSOCV, we found 11 signal features $C_1 - C_{11}$ believed to well explain the impact of the FMTPA on foot motions while excluding individual differences and data bias. In most biomedical engineering studies, the number of participants is never large, so it is difficult to cover the variation of all hidden individual factors, e.g., lifestyle habits, medical history, and profession. We considered only including intrinsic features of the human body and the estimation model should be robust against individual difference despite the small number of samples. Therefore, we discuss the following findings that might be related to previous biomechanical findings.

The impact of the FMTPA was observed in MSt (c_1, c_2, c_6, c_7, and c_{10}), TSt (c_5, c_8, and c_9), PS (c_4 and c_9), periods immediately after an HS and TO (c_3, c_9, and c_{11}), and MSw (c_3 and c_9), which is very similar to the results shown in the report of Deschamps *et al.* [24].

Despite the signal amplitude being very near zero during foot flats in the coronal plane, the impact of the FMTPA on foot motion was still observed thanks to the high signal-to-noise ratio of the IMS. By observing C_1, C_2, C_5, C_6, and C_{10} as the FMTPA increased, the foot motion gradually became a mirror inversion. Throughout MSt, the feet with low FMTPAs initially had an inversion posture. The feet were then further supinated during the first half and pronated back during the second half (C_1, C_5, and C_{10}). However, those with high FMTPAs started at an eversion posture, were further pronated, then supinated back (C_2, C_6, and C_{10}). These results might be related to the supporting point of the foot sole shifting due to the eversion deviation in the subtalar joint alignment in people with HV, as reported in a previous study [26].

The most affected periods are TSt and PS, where the vertical ground reaction force rises above the resting body weight and the center of pressure moves from forefoot to big toe [24]. We observed that high-FMTPA participants tended to rotate more in the eversion direction and had a posture having a more sole-to-ground eversion angle during TSt and PS (C_7 and C_{11}). This might suggest that the foot is forced to evert more to keep balance before TO due to the support-point alteration induced by increasing the FMTPA [26].

An increasing FMTPA decreases both in the hindfoot-tibia dorsiflexion angle throughout the entire GC and decreases in the tibia-ground forward angle from TSt to ISw [25], [26], which was the reason for E_x increasing throughout TSt to MSw (C_9) observed in higher-FMTPA participants. The E_x could be obtained by summing the hindfoot-tibia and tibia-ground angle in the sagittal plane.

We also found that several new FMTPA-impacted gait features might only exist in inertial signals. We first observed that a significant change in foot motion occurred along the coronal plane of high-FMTPA participants, reducing their pronated rotational velocity or even making it inverse to a supinated rotation during late ISw (C_8). We then observed an earlier peak occurrence during LR (c_3) in A_z as the FMTPA increased. This finding suggested that high-FMTPA participants tended to drop their foot sole fast and hard, inducing strong impact on the foot sole during walking. This might negatively affect the foot arch muscles and induce foot arch collapse, which is a causative factor of HV [39]–[41]. Finally, an earlier signal rise in G_x and in E_x during a TSt along with an increase in FMTPA (c_4 and early c_9) suggested earlier HR in high-FMTPA participants.

Despite these valuable findings, we have to acknowledge certain limitations which are subject to discussion. HV is also a common foot deformity in children, adolescents, and the elderly [42]–[44], whereas the ages of the participants in this study were limited between 20 and 60. Because the skeleton and muscles of children and adolescents are still developing, their gait differs from adults [45], while the kinematic features of the elderly differ from those of younger people due to age-related muscles weakness [46], [47]. Regarding the elderly, gait changes may impact the significant signal features for FMTPA estimation, for example, c_3 located at the phase immediately after HS when the quadriceps are activated during walking [23]. Therefore, the age-related weakness of quadriceps may also impact the foot motion at this phase while generating crosstalk on this FMTPA-related feature. More data of much younger and more elderly participants should be included in the future.

Rather than embedding an IMS into the sole of a shoe, our design of embedding an IMS into insoles enables various types of shoes to be used. However, we only studied the wearing of sports shoes. According to previous studies, gait can be altered when wearing different shoes, especially high-heeled shoes [48], [49], which were considered as significant extrinsic factors of female HV progression [21]. The foot sizes of children and adolescents are commonly below 20 cm. Since the length of our IMS along the longitude axis of the foot is 3.5 cm, it may exceed the range of their foot arch, thus will more or less affect comfort. Further discussion on wearing different types of shoes and how to improve the design of the IMS to fit the needs of children and adolescents is still needed.

Another limitation is that we assumed two feet have symmetric foot motions. Previous studies suggested a difference in gait between the dominant and non-dominant foot [50]. Whether the difference will significantly impact the estimation model requires further discussion, particularly for those users whose lower limbs and gait are asymmetric.

Since there are foot problems involving foot motion deviating from normal cases, not only HV by using an IMS, but detecting deformities of other parts of the foot, e.g. over-pronation [51] or flat footedness, should also be investigated. An over-pronated foot is induced by abnormal subtalar joint alignment and considered an intrinsic risk factor for developing lower extremity injury [52]. Through analyzing different parts of the foot, users can be advised to change to a more appropriate shoe to avoid HV or purchase motion-control shoes and/or insoles to correct over-pronated feet [53].

VI. Conclusion

We constructed an FMTPA estimation model using IMS signal features and machine-learning methods. This was the first time investigating the impact of the FMTPA on foot motion, especially inertial signals, and found 11 effective predictors existing in all GCPs except the terminal swing. Our model constructed using linear regression was found to be the best, achieving an RMSE of 4.2 degrees. Our results had good agreement with the true values, which demonstrated the possibility of FMTPA measurement as well as of daily foot-health monitoring by using an IMS. For future work, we will investigate whether an interactive factor between FMTPA and footwear exist to construct a more reliable model for practical use and test the applicability of the model for the elderly and people with neuromuscular or orthopedic disease in a clinical setting. We will also investigate whether there are better machine-learning methods to achieve better estimation.

Acknowledgment

The authors thank their colleagues of NEC Corporation for their help during the data collection.

References

[1] B. Reeder and A. David, "Health at hand: A systematic review of smart watch uses for health and wellness," *J. Biomed. Informat.*, vol. 63, pp. 269–276, Oct. 2016, doi: 10.1016/j.jbi.2016.09.001.

[2] M. Chung, G. Fortunato, and N. Radacsi, "Wearable flexible sweat sensors for healthcare monitoring: A review," *J. Roy. Soc. Interface*, vol. 16, no. 159, Oct. 2019, Art. no. 20190217, doi: 10.1098/rsif.2019.0217.

[3] A. G. Leal-Junior, C. A. R. Diaz, L. M. Avellar, M. J. Pontes, C. Marques, and A. Frizera, "Polymer optical fiber sensors in healthcare applications: A comprehensive review," *Sensors*, vol. 19, no. 14, p. 3156, Jul. 2019, doi: 10.3390/s19143156.

[4] F. M. Rast and R. Labruyère, "Systematic review on the application of wearable inertial sensors to quantify everyday life motor activity in people with mobility impairments," *J. NeuroEng. Rehabil.*, vol. 17, no. 1, pp. 1–19, Dec. 2020, doi: 10.1186/s12984-020-00779-y.

[5] A. G. Leal-Junior, A. Frizera, L. M. Avellar, C. Marques, and M. J. Pontes, "Polymer optical fiber for in-shoe monitoring of ground reaction forces during the gait," *IEEE Sensors J.*, vol. 18, no. 6, pp. 2362–2368, Mar. 2018, doi: 10.1109/JSEN.2018.2797363.

[6] A. G. Leal-Junior, C. R. Díaz, C. Marques, M. J. Pontes, and A. Frizera, "3D-printed POF insole: Development and applications of a low-cost, highly customizable device for plantar pressure and ground reaction forces monitoring," *Opt. Laser Technol.*, vol. 116, pp. 256–264, Aug. 2019, doi: 10.1016/j.optlastec.2019.03.035.

[7] A. G. Leal, Jr., C. A. R. Díaz, A. Frizera, C. Marques, M. R. N. Ribeiro, and M. J. Pontes, "Simultaneous measurement of pressure and temperature with a single FBG embedded in a polymer diaphragm," *Opt. Laser Technol.*, vol. 112, pp. 77–84, Apr. 2019, doi: 10.1016/j.optlastec.2018.11.013.

[8] D. Gokalgandhi, L. Kamdar, N. Shah, and N. Mehendale, "A review of smart technologies embedded in shoes," *J. Med. Syst.*, vol. 44, no. 9, pp. 1–9, Sep. 2020, doi: 10.1007/s10916-020-01613-7.

[9] B. Eskofier *et al.*, "An overview of smart shoes in the Internet of Health Things: Gait and mobility assessment in health promotion and disease monitoring," *Appl. Sci.*, vol. 7, no. 10, p. 986, Sep. 2017, doi: 10.3390/app7100986.

[10] B. Mariani, S. Rochat, C. J. Büla, and K. Aminian, "Heel and toe clearance estimation for gait analysis using wireless inertial sensors," *IEEE Trans. Biomed. Eng.*, vol. 59, no. 11, pp. 3162–3168, Nov. 2012, doi: 10.1109/TBME.2012.2216263.

[11] M. O'Reilly, B. Caulfield, T. Ward, W. Johnston, and C. Doherty, "Wearable inertial sensor systems for lower limb exercise detection and evaluation: A systematic review," *Sports Med.*, vol. 48, no. 5, pp. 1221–1246, May 2018, doi: 10.3390/s101211556.

[12] A. Baghdadi, L. A. Cavuoto, A. Jones-Farmer, S. E. Rigdon, E. T. Esfahani, and F. M. Megahed, "Monitoring worker fatigue using wearable devices: A case study to detect changes in gait parameters," *J. Qual. Technol.*, vol. 53, no. 1, pp. 47–71, 2019, doi: 10.1080/00224065.2019.1640097.

[13] M. J. Mohler, C. S. Wendel, R. E. Taylor-Piliae, N. Toosizadeh, and B. Najafi, "Motor performance and physical activity as predictors of prospective falls in community-dwelling older adults by frailty level: Application of wearable technology," *Gerontology*, vol. 62, no. 6, pp. 654–664, 2016, doi: 10.1159/000445889.

[14] Pardoel, Kofman, Nantel, and Lemaire, "Wearable-sensor-based detection and prediction of freezing of gait in Parkinson's disease: A review," *Sensors*, vol. 19, no. 23, p. 5141, Nov. 2019, doi: 10.3390/s19235141.

[15] P. Palomo-López *et al.*, "Quality of life related to foot health status in women with fibromyalgia: A case-control study," *Arch. Med. Sci.*, vol. 15, no. 3, pp. 694–699, 2019, doi: 10.5114/aoms.2018.77057.

[16] A. Reinoso-Cobo *et al.*, "Foot health and quality of life in patients with rheumatoid arthritis: A cross-sectional study," *BMJ Open*, vol. 10, no. 5, May 2020, Art. no. e036903, doi: 10.1136/bmjopen-2020-036903.

[17] D. Lopez Lopez *et al.*, "Foot health-related quality of life among elderly with and without lesser toe deformities: A case–control study," *Patient Preference Adherence*, vol. 12, pp. 251–255, Feb. 2018, doi: 10.2147/PPA.S152269.

[18] L. Wang *et al.*, "A review of wearable sensor systems to monitor plantar loading in the assessment of diabetic foot ulcers," *IEEE Trans. Biomed. Eng.*, vol. 67, no. 7, pp. 1989–2004, Jul. 2020, doi: 10.1109/TBME.2019.2953630.

[19] C. S. Thorne, A. Gatt, C. DeRaffaele, A. Bazena, and C. Formosa, "Digital foot health technology and diabetic foot monitoring: A systematic review," *Diabetes Res. Clin. Pract.*, vol. 175, May 2021, Art. no. 108783, doi: 10.1016/j.diabres.2021.108783.

[20] T. W. Kernozek, A. Elfessi, and S. Sterriker, "Clinical and biomechanical risk factors of patients diagnosed with hallux valgus," *J. Amer. Podiatric Med. Assoc.*, vol. 93, no. 2, pp. 97–103, Mar. 2003, doi: 10.7547/87507315-93-2-97.

[21] H. B. Menz, E. Roddy, E. Thomas, and P. R. Croft, "Impact of hallux valgus severity on general and foot-specific health-related quality of life," *Arthrit. Care Res.*, vol. 63, no. 3, pp. 396–404, 2011, doi: 10.1002/acr.20396.

[22] H. Piggott, "The natural history of hallux valgus in adolescence and early adult life," *J. Bone Joint Surg. Brit.*, vol. 42-B, no. 4, pp. 749–760, Nov. 1960, doi: 10.1302/0301-620X.42B4.749.

[23] D. A. Neumann, *Kinesiology of the Musculoskeletal System: Foundations of Physical Rehabilitation*, 2nd ed. St Louis, MO, USA: Mosby, 2010, pp. 627–699.

[24] S. E. Nix, B. T. Vicenzino, N. J. Collins, and M. D. Smith, "Gait parameters associated with hallux valgus: A systematic review," *J. Foot Ankle Res.*, vol. 6, no. 1, pp. 1–12, Dec. 2013, doi: 10.1186/1757-1146-6-9.

[25] K. Deschamps, I. Birch, K. Desloovere, and G. A. Matricali, "The impact of hallux valgus on foot kinematics: A cross-sectional, comparative study," *Gait Posture*, vol. 32, no. 1, pp. 102–106, May 2010, doi: 10.1016/j.gaitpost.2010.03.017.

[26] J. Miroslav, C. Lee, S. Zdenek, K. Jitka, and G. Anna, "Kinematic analysis of gait in patients with juvenile hallux valgus deformity," *J. Biomech. Sci. Eng.*, vol. 3, no. 3, pp. 390–398, 2008, doi: 10.1299/jbse.3.390.

[27] K. Canseco, L. Rankine, J. Long, T. Smedberg, R. M. Marks, and G. F. Harris, "Motion of the multisegmental foot in hallux valgus," *Foot Ankle Int.*, vol. 31, no. 2, pp. 146–152, 2010, doi: 10.3113/2FFAI.2010.0146.

[28] C. Huang *et al.*, "The impact of first metatarsophalangeal angle on the gait features measured by an in-shoe motion sensor," in *Proc. IEEE Sensors*, Oct. 2020, pp. 1–4, doi: 10.1109/SENSORS47125.2020.9278703.

[29] J. Velotta, J. Weyer, A. Ramirez, J. Winstead, and R. Bahamonde, "Relationship between leg dominance tests and type of task," *Biomech. Spor.*, vol. 29, no. 11, pp. 1035–1039, 2010. [Online]. Available: https://www.researchgate.net/publication/236649977Relationshipbetweenlegdominanceandtypeoftask

[30] S. O. H. Madgwick, A. J. L. Harrison, and R. Vaidyanathan, "Estimation of IMU and MARG orientation using a gradient descent algorithm," in *Proc. IEEE Int. Conf. Rehabil. Robot.*, Jun. 2011, pp. 1–7, doi: 10.1109/ICORR.2011.5975346.

[31] S. Nix, T. Russell, B. Vicenzino, and M. Smith, "Validity and reliability of hallux valgus angle measured on digital photographs," *J. Orthopaedic Sports Phys. Therapy*, vol. 42, no. 7, pp. 642–648, Jul. 2012, doi: 10.2519/jospt.2012.3841.

[32] C. Huang, K. Fukushi, Z. Wang, H. Kajitani, F. Nihey, and K. Nakahara, "Initial contact and toe-off event detection method for in-shoe motion sensor," in *Activity and Behavior Computing. Smart Innovation, Systems and Technologies*, vol. 204, M. A. R. Ahad, S. Inoue, D. Roggen, K. Fujinami, Eds. Singapore: Springer, 2021, pp. 101–118, doi: 10.1007/978-981-15-8944-7_7.

[33] D. Sun, G. Fekete, Q. Mei, and Y. Gu, "The effect of walking speed on the foot inter-segment kinematics, ground reaction forces and lower limb joint moments," *PeerJ*, vol. 6, Aug. 2018, Art. no. e5517. [Online]. Available: https://www.ncbi.nlm.nih.gov/pubmed/30155372

[34] A. Hartmann, S. Luzi, K. Murer, R. A. de Bie, and E. D. de Bruin, "Concurrent validity of a trunk tri-axial accelerometer system for gait analysis in older adults," *Gait Posture*, vol. 29, no. 3, pp. 444–448, Apr. 2009, doi: 10.1016/j.gaitpost.2008.11.003.

[35] C. Piqué-Vidal and J. Vila, "A geometric analysis of hallux valgus: Correlation with clinical assessment of severity," *J. Foot Ankle Res.*, vol. 2, no. 1, pp. 1–8, Dec. 2009, doi: 10.1186/1757-1146-2-15.

[36] T. E. Kilmartin, R. L. Barrington, and W. A. Wallace, "The X-ray measurement of hallux valgus: An inter-and intra-observer error study," *The Foot*, vol. 2, no. 1, pp. 7–11, 1992, doi: 10.3113/2FFAI.2010.0146.

[37] F. Hoflinger, J. Müller, R. Zhang, L. M. Reindl, and W. Burgard, "A wireless micro inertial measurement unit (IMU)," *IEEE Trans. Instrum. Meas.*, vol. 62, no. 9, pp. 2583–2595, Sep. 2013, doi: 10.1109/TIM.2013.2255977.

[38] B. Sensortec, *Data Sheet: BMI 160, Small, Low Power Inertial Measurement Unit*, document BST-BMI160-DS000-09, 2020. [Online]. Available: https://www.bosch-sensortec.com/media/boschsensortec/downloads/datasheets/bst-bmi160-ds000.pdf

[39] A. M. Perera, L. Mason, and M. M. Stephens, "The pathogenesis of hallux valgus," *J. Bone Joint Surg.*, vol. 93, no. 17, pp. 1650–1661, Sep. 2011, doi: 10.2106/JBJS.H.01630.

[40] S. Eustace, J. O. Byrne, O. Beausang, M. Codd, J. Stack, and M. M. Stephens, "Hallux valgus, first metatarsal pronation and collapse of the medial longitudinal arch ? A radiological correlation," *Skeletal Radiol.*, vol. 23, no. 3, pp. 191–194, Apr. 1994, doi: 10.1007/BF00197458.

[41] J. Dygut *et al.*, "Correction of foot deformities with hallux valgus by transversal arch restoration," *Biocybernetics Biomed. Eng.*, vol. 40, no. 4, pp. 1556–1567, Oct. 2020, doi: 10.1016/j.bbe.2020.09.006.

[42] J. R. Davids, T. A. Mason, A. Danko, D. Banks, and D. Blackhurst, "Surgical management of hallux valgus deformity in children with cerebral palsy," *J. Pediatr. Orthopaed.*, vol. 21, no. 1, pp. 89–94, 2001, doi: 10.1097/00004694-200101000-00018.

[43] Z. Harb, M. Kokkinakis, H. Ismail, and G. Spence, "Adolescent hallux valgus: A systematic review of outcomes following surgery," *J. Children's Orthopaedics*, vol. 9, no. 2, pp. 105–112, Apr. 2015, doi: 10.1007/s11832-015-0655-y.

[44] U.-S.-D. T. Nguyen *et al.*, "Factors associated with hallux valgus in a population-based study of older women and men: The MOBILIZE Boston study," *Osteoarthritis Cartilage*, vol. 18, no. 1, pp. 41–46, Jan. 2010, doi: 10.1016/j.joca.2009.07.008.

[45] K. J. Ganley and C. M. Powers, "Gait kinematics and kinetics of 7-year-old children: A comparison to adults using age-specific anthropometric data," *Gait Posture*, vol. 21, no. 2, pp. 141–145, 2005, doi: 10.1016/j.gaitpost.2004.01.007.

[46] D. Hamacher, N. B. Singh, J. H. Van Dieën, M. O. Heller, and W. R. Taylor, "Kinematic measures for assessing gait stability in elderly individuals: A systematic review," *J. Roy. Soc. Interface*, vol. 8, no. 65, pp. 1682–1698, Dec. 2011, doi: 10.1098/rsif.2011.0416.

[47] A. Mika, Ł. Oleksy, P. Mika, A. Marchewka, and B. C. Clark, "The influence of heel height on lower extremity kinematics and leg muscle activity during gait in young and middle-aged women," *Gait Posture*, vol. 35, no. 4, pp. 677–680, Apr. 2012, doi: 10.1016/j.gaitpost.2011.12.001.

[48] C. Morio, M. J. Lake, N. Gueguen, G. Rao, and L. Baly, "The influence of footwear on foot motion during walking and running," *J. Biomechanics*, vol. 42, no. 13, pp. 2081–2088, Sep. 2009, doi: 10.1016/j.jbiomech.2009.06.015.

[49] N. J. Cronin, "The effects of high heeled shoes on female gait: A review," *J. Electromyogr. Kinesiol.*, vol. 24, no. 2, pp. 258–263, Apr. 2014, doi: 10.1016/j.jelekin.2014.01.004.

[50] D. W.-C. Wong, W.-K. Lam, and W. C.-C. Lee, "Gait asymmetry and variability in older adults during long-distance walking: Implications for gait instability," *Clin. Biomech.*, vol. 72, pp. 37–43, Feb. 2020, doi: 10.1016/j.clinbiomech.2019.11.023.

[51] C. Huang, Z. Wang, K. Fukushi, F. Nihey, H. Kajitani, and K. Nakahara, "Assessment of over-pronated/over-supinated foot using foot-motion measured by an in-shoe motion sensor," in *Proc. IEEE Biomed. Circuits Syst. Conf. (BioCAS)*, 2021, pp. 1–6, doi: 10.1109/BioCAS49922.2021.9644969.
[52] H. B. Menz, A. B. Dufour, J. L. Riskowski, H. J. Hillstrom, and M. T. Hannan, "Association of planus foot posture and pronated foot function with foot pain: The Framingham foot study," *Arthritis Care Res.*, vol. 65, no. 12, pp. 1991–1999, Dec. 2013, doi: 10.1002/acr.22079.
[53] H. A. Banwell, S. Mackintosh, D. Thewlis, and K. B. Landorf, "Consensus-based recommendations of Australian podiatrists for the prescription of foot orthoses for symptomatic flexible pes planus in adults," *J. Foot Ankle Res.*, vol. 7, no. 1, pp. 1–13, Dec. 2014, doi: 10.1186/s13047-014-0049-2.

Chenhui Huang (Member, IEEE) received the B.S. degree in optical engineering from the Harbin Institute of Technology, China, in 2009, and the M.S. and Ph.D. degrees in biomedical engineering from Tohoku University, Japan, in 2012 and 2015, respectively.

He joined the Center Research Labs, NEC Corporation, in 2015. Initially, his work concerned remote sensing technology using quantum dot infrared photodetector. In 2018, he started working on the healthcare technologies based on daily gait analysis. His current research interests include biomechanical analysis on gait, gait analysis and its application for daily healthcare, and activity monitoring using motion sensors, especially the sensor mounted on foot, involving the use of signal processing and machine learning. He is a member of SPIE, The Institute of Electronics, Information and Communication Engineers of Japan, and the Japanese Society of Applied Physics.

Kenichiro Fukushi received the B.Eng., M.Eng., and D.Eng. degrees in information processing from the Tokyo Institute of Technology, Japan, in 2003, 2009, and 2014, respectively. From 2010 to 2012, he was a visiting student at the MIT Media Lab, USA. In 2013, he joined NEC Corporation, Japan, where he is currently a Research Manager. His research interests include wearable sensing, machine learning, computer vision, and computational photography. Dr. Fukushi is a member of the Institute of Electronics, Information and Communication Engineers, Japan.

Zhenwei Wang received the B.S. and M.S. degrees from the Department of Mechanical Systems Engineering, Tokyo City University, Japan, in 2014 and 2016, respectively. He joined the Center Research Labs, NEC Corporation, in 2016. Initially, he was involved in drone research and development. Until 2020, he was researching and developing autonomous flight of drones by model predictive control and self-position estimation by V-SLAM. He now started working on the healthcare technologies based on gait analysis to contribute to the medical and long-term care fields by performing gait analysis using motion capture and IMU sensors.

Hiroshi Kajitani received the B.S. and M.S. degrees in electrical engineering from Kyoto University, Japan, in 1986 and 1988, respectively. He joined the Center Research Labs, NEC Corporation, in 1988. His work concerned about the magnetic recording, the 3D MEMS optical switches, and the fuel cell systems for portable electric devices from 1988 to 2016. In 2017, he started working on healthcare technologies, especially low power IoT sensors for monitoring human information and now developing gait monitoring sensors. He is a member of the Japanese Society of Applied Physics, the Japan Society of Mechanical Engineers, and the Robotics Society of Japan.

Fumiyuki Nihey received the M.S. and Ph.D. degrees in physics from Osaka University, Japan, in 1987 and 1996, respectively. In 1987, he joined the Central Research Labs, NEC Corporation, where he engaged in fundamental research on microelectronics and nanotechnology. In 2020, he joined a research group on healthcare technology based on gait analysis. His current research interests include biomechanical analysis of gait, its application to daily healthcare, and activity monitoring of the elderly using foot motion sensors. He is a member of the Japan Society of Applied Physics.

Hannah Pokka received the B.S. degree in communications engineering from Dalian University in 2010 and the M.S. degree in materials science from Tohoku University in 2013. She joined the NEC Telecommunication Division in 2013. She entered healthcare field in 2018 and started working on business design of gait sensing technology. Her responsibilities have included developing the business model, customer development, and designing the demonstration.

Hiroko Narasaki received the master's degree in design from the Kyoto Institute of Technology in 2017. She joined the Corporate Business Development Division, NEC Corporation, in 2017. She works as a member of project teams for new business development and designs new services. In 2018, she joined a healthcare project team and designed service and related products of insole-embedded smart motion sensor.

Hiroaki Nakano received the B.S. degree in economics from Keio University. He joined NEC Corporation in 2006 and initially his work concerned new solution development for financial institutions. After two years of job experiences in Nomura Securities from 2009 to 2011, he started to be in charge of new business development in the AI-related and healthcare fields. His current challenge is to develop a wellness solution with the theme of "visualization of invisible health condition" through monitoring daily walking and to explore new services with business partners.

Kentaro Nakahara received the B.S. and M.S. degrees from the Department of Applied Chemistry, University of Tokyo, in 1997 and 1999, respectively, and the Ph.D. degree from the Graduate School of Advanced Science and Engineering, Waseda University, in 2011. He joined NEC Corporation in 1999 and had been engaged in the research for rechargeable batteries for over the decade. He is now broadly interested in applied research in the healthcare field of advanced artificial intelligence and the IoT technologies, managing research such as gait analysis and stress estimation technologies. His representative research achievement is the discovery of a new type of rechargeable battery named "Organic Radical Battery," and for this achievement he has received the 10th Green Sustainable Chemistry (GSC) Award, the 17th Chemistry and Bio-Technology Tsukuba Award, and 2009 Young Scientists Award from Minister of Education, Culture, Sports, Science and Technology.